Surfactant–Polymer Flooding

Druetta, Pablo; Picchioni, Francesco

Published in:
Energy & fuels

DOI:
10.1021/acs.energyfuels.8b02900

Publication date:
2018

energy&fuels

Article

Cite This: Energy Fuels 2018, 32, 12231−12246

pubs.acs.org/EF

Surfactant−Polymer Flooding: Influence of the Injection Scheme

Pablo Druetta and Francesco Picchioni*

Department of Chemical Engineering, ENTEG, University of Groningen, Nijenborgh 4, 9747AG Groningen, The Netherlands

Supporting Information

ABSTRACT: The use of standard enhanced oil recovery (EOR) techniques allows for the improvement of oilfield performance after waterflooding processes. Chemical EOR methods modify different properties of fluids and/or rock to mobilize the remaining oil. Moreover, combined techniques have been developed to maximize the performance by using the joint properties of the chemical slugs. A new simulator is presented to study a surfactant−polymer flooding, based on a two-phase, five-component system (aqueous and oleous phases with water, petroleum, polymer, surfactant, and salt) for a 2D reservoir model. The physical properties modified by these chemicals are considered as well as the synergy between them. The analysis of the chemical injection strategy is deemed vital for the success of the operations. This plays a major role in the efficiency of the recovery process, including the order and the time gap between each chemical slug injection. As the latter is increased, the flooding tends to behave as two separate processes. Best results are found when both slugs are injected overlapped, with the polymer in first place which improves the sweeping efficiency of the viscous oil. This simulator can be used to study different chemical combinations and their injection procedure to optimize the EOR process.

INTRODUCTION

During the last 150 years the world economy has depended on different energy sources. Crude oil and its derivatives have represented during this period the main source of energy, and even though new and more environmentally friendly sources are being developed, the economy is not ready to stop relying on the former.[1−10] The exploitation of an oil field goes through different stages, based on the mechanisms involved in the sweeping process:[11,12] during primary recovery, oil is driven by natural mechanisms, and subsequently, during secondary recovery, water is usually injected to repressurize the field and sweep part of the trapped oil to the producing wells. However, after these two stages, more than 50% of the original oil in place (OOIP) still remains trapped.[13,14] Considering also the facts that the discovery of new fields has steadily decreased during the last 30 years and the demand of energy increases yearly, the only available option is to maximize the performance of existing, mature fields. Tertiary oil recovery or EOR processes aim at this. Among these, the combined use of chemical agents present great potential since it takes advantage of the different mechanisms affected by the presence of these species in the injection fluid. Hence, in this study the combined technique, polymer and surfactant, including also their synergy and interactions in the porous medium, is proposed. The objective of this paper is then to present a novel simulator for a two-phase, five-component model, including the analysis of the injection procedure, presenting different time gaps between chemical slugs in order to draw conclusions about how to maximize the recovery factor.[6,11,14−16]

Polymer−Surfactant Flooding. A surfactant/polymer process cannot be considered as two independent processes, taking place at the same time in the reservoir. The synergy of both chemicals affects the recovery factor. However, the transport of each of these substances influences to a greater or lesser extent the other, and vice versa. This compatibility has already been presented by several authors in numerical simulations as well as in laboratory tests.[17−23] This phenomenon is known as surfactant−polymer interaction or incompatibility (SPI), and it is well described by Sheng.[13] According to him, the compatibility between both products is a subject to be especially considered, as well as the injection strategy. If the polymer is injected before the surfactant, the former acts as a "sacrificial agent" to prevent excessive adsorption or for conformance improvement. Conversely, if the injection strategy is the opposite, the phenomenon of water fingering is avoided in the surfactant slug. This interaction must always be considered in the porous medium because, although both products may not be injected at the same time, by dispersion and diffusion phenomena, they will be mixed during the sweeping process. Even if both dispersion and diffusion of the chemical components are considered negligible and the polymer is injected behind the surfactant, the mixing process will take place due to the phenomenon of inaccessible volume (IAPV). One of the most noticeable effects in this interaction is seen in the measurement of IFT as a function of polymer and surfactant concentrations. When the former is introduced into the system, the critical micelle concentration (CMC) is replaced by two different values (Figure 1), namely, the critical aggregation concentration (CAC), lower than the CMC, at which surfactant molecules start to adsorb and interact with the polymer chains, and the polymer saturation point (PSP), higher than the CMC, which is the surfactant concentration at which micelles are formed when polymer molecules are present.[24]

Beyond the adopted injection strategy, the presence of the polymer in the surfactant slug is considered fundamental in order to maintain a suitable mobility ratio and thus avoid

Received: August 21, 2018
Revised: October 30, 2018
Published: October 30, 2018

DOI: 10.1021/acs.energyfuels.8b02900
Energy Fuels 2018, 32, 12231−12246

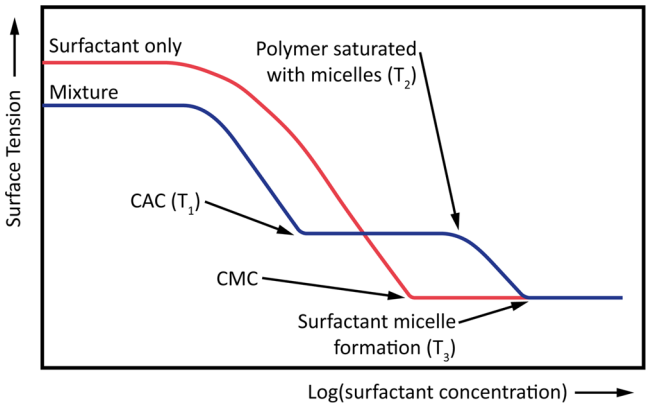

Figure 1. Effect of the polymer on the IFT.

fingering phenomena.[13] This "double" injection of polymer improves the process sweeping efficiency, reducing the residual oil saturation. As mentioned earlier, this novel simulator considers in addition to the chemicals the presence of the salt in the porous medium. The latter affects in a different way both products: the presence of salt decreases the viscosifying properties of the polymer, whereas the efficiency of the process with surfactants depends on the concentration of salt and the critical salinity values of the surfactant used.[13,25−27]

The influence on the recovery process has also been thoroughly discussed.[19,28−38] Laboratory results have shown that in both heterogeneous and homogeneous media, the synergism of the polymer plus the surfactant improves the sweeping efficiency, even though the IFT values are higher in the case of surfactant alone.[13] It has been shown that a combined flooding process improves sweeping results as compared to traditional methods of chemical EOR. However, it is critical to determine the SP flooding starting point. It has been demonstrated in trials as well as in simulations that the results of EOR recoveries depend on the moment when the process begins. Optimum results are obtained when the EOR flooding starts as soon as possible, often without traditional waterflooding or secondary recovery processes. The simulations show that the previous waterflooding does not increase the final value, but increases the operating time and slightly decreases the recovered oil. Thus, it is considered that the chemical flood should be started at higher oil saturations. However, as already mentioned, this is not usually done in practice due to several reasons: (1) an early and cheaper waterflooding is deemed necessary for the reservoir characterization in order to reduce the uncertainties concerning the porous medium; (2) any chemical flooding process requires longer preparation time, including laboratory study and more complex facilities; (3) more technical skills and competence are needed to run a chemical flood project; and (4) since the money invested is substantially higher, more time is needed to get the project approved by companies.

Aim of this Work. The goal in this paper is to present a novel simulator in a two-dimensional oil field, capable of simulating the flow of a two-phase, five-component system in a combined surfactant−polymer flooding. The surfactant's component partitioning is modeled in an accurate, yet relatively simple and robust way, using a ternary diagram. The polymer module includes a complete degradation system based on the molecular weight, which affects both the viscoelastic and rheological properties of the solution. The presence of a fifth component, monovalent salt, also influences the properties of surfactant and polymer. The salt content is expressed as a function of the total dissolved solids (TDS) present only in the water phase, using a function based on the literature. This will lead to a new set of optimum design parameters to be used during the synthesis of future surfactants and polymers. The combination of the mentioned factors has resulted in a novel and complete simulator, which can be used for the design of combined SP flooding. The compositional flow model was adopted due to the fact that it offers a suitable and relatively easy approach to study chemical EOR processes, which can be described in terms of the mass transfer of a number of components (e.g., polymers, surfactants, salt, etc.) in two- or three-phase systems. The objective in this present study is to present this simulator, studying the combined effect of polymer and surfactants and focusing on the injection scheme, in order to find the optimum in terms of oil recovered. This is coupled in the second part with a secondary recovery, so as to determine the best moment to start the EOR operations.

Physical Model. The two-dimensional oil field reservoir used in this paper is based on a geometric pattern usually found in the oil industry. The five-spot scheme consists of a square domain, with constant or variable properties, where an injection well is placed at the center and four producing points are located at the corners. During this analysis, a simplification of the model was performed in what is known as the quarter five-spot. The physical model is represented then by a 2D reservoir (Ω) of known physical and geometrical properties which has an absolute permeability tensor (K) and a porosity field (ϕ), which can be constant or represented by normal distribution functions. Moreover, the porosity may be also affected by the rock compressibility (Figure 2).

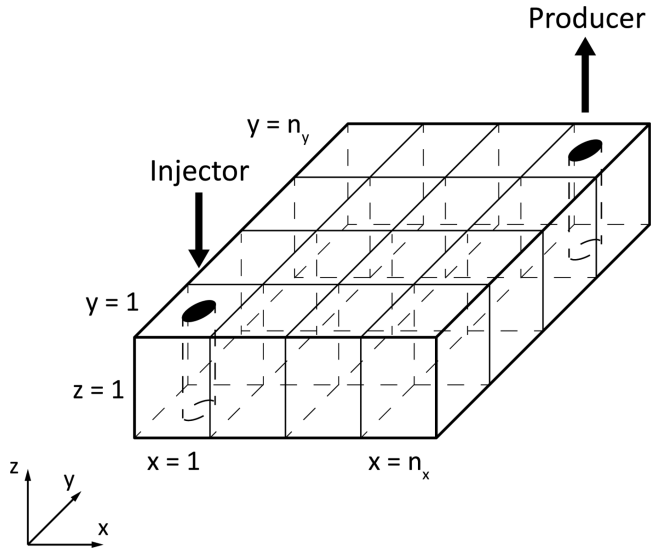

Figure 2. Schematic representation of the 2D reservoir using the quarter five-spot configuration.[43]

The flow is assumed to be isothermal, Newtonian for the oleous phase, and incompressible, and it is considered that the vertical permeability is negligible compared to horizontal components of the tensor; it is also considered that the system is in local thermodynamic (phase) equilibrium. Since it is considered on a macroscopic field-scale, Darcy's law is valid, and moreover, the gravitational forces are negligible when compared to the viscous and capillary ones.[39]

Surfactant/polymer EOR flooding involves the flow of fluids in a two-phase (aqueous and oleous), multicomponent (water,

DOI: 10.1021/acs.energyfuels.8b02900
Energy Fuels 2018, 32, 12231−12246

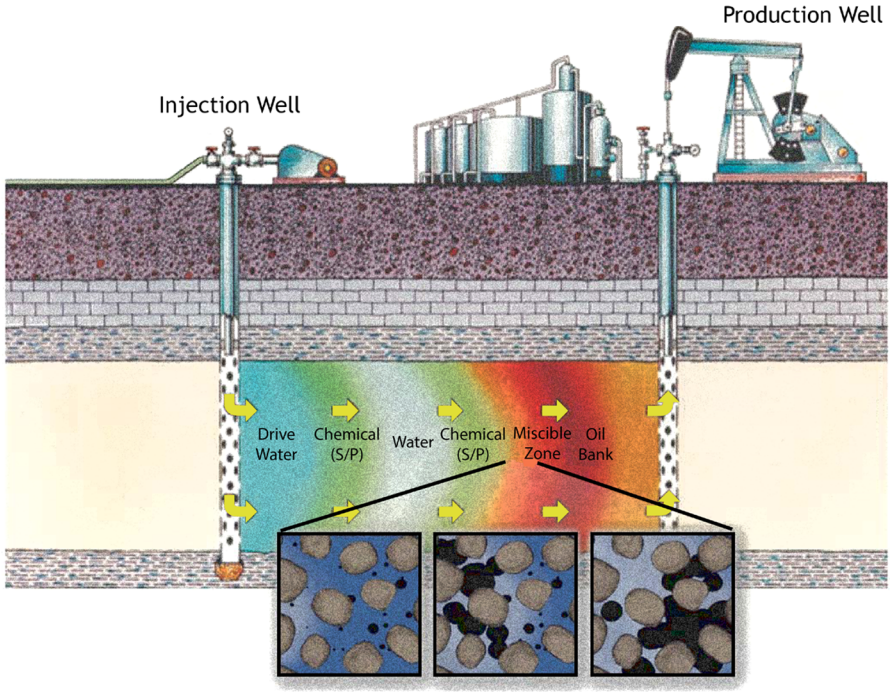

Figure 3. Scheme of a combined chemical EOR flooding, simplified to a 1D representation (adapted from Sweatman[40]).

salt, polymer, surfactant, and petroleum) system. The properties of the polymer are determined by its average molecular weight, assuming that all the molecules are identical, which means the polydispersity index (PDI) is equal to unity. In reality, there is a probability density function (considered to be Gaussian) of the molecular weight, based on the variability of the molecules' length (PDI > 1). The recovery process involves injecting in a first stage an aqueous solution with the polymer/surfactant, followed by a surfactant/polymer slug, driven by a water bank (water or brine) and mobilizing the oil into the producing wells (Figure 3).

The model is represented by a system of strongly nonlinear partial differential equations, complemented by a set of algebraic relationships describing physical properties of the fluid and the rock, namely, component partitioning as a function of the salinity, interfacial tension, residual phase saturations, relative permeabilities, rock wettability, phase viscosities, capillary pressure, adsorption of both polymer and surfactant onto the formation, inaccessible pore volume (IAPV), disproportionate permeability reduction (DPR), surfactant−polymer interactions (SPI), and dispersion. The numerical technique adopted for the resolution of these equations is the IMPEC method, which calculates pressures implicitly and concentration for each of the components explicitly. By improving the discretization methods presented in the literature,[41,42] a fully second-order accuracy scheme is adopted in the model with flux limiter functions implemented in order to track more accurately the components throughout the reservoir and minimize the influence of numerical diffusion phenomena.

Mathematical Model. The system of equations to model a multiphase, multicomponent system in porous media under a continuum approach is well-known from the literature. The compositional model offers the versatility to study the transport of a number chemical species in porous media, which might affect the fluid and/or rock properties. However, increasing the number of components increases the auxiliary algebraic relationships necessary to determine numerically the system of equations. In the case of SP flooding in a five-component, two-phase system, a number of $N_{comp}(N_{phases} - 1) = 5$ auxiliary relationships is needed, which are determined by the system phase behavior. Based on Figure 2, the model is aimed at studying the full reservoir-scale, dividing the domain in representative elementary volumes (REVs) in which the physical properties are assumed to be constant.

This simulator is based originally on an upwind, first-order 2D compositional simulator aimed at studying surfactant EOR processes,[43] which was validated against commercial and academic simulators in a series of 2D flooding processes (UTCHEM and GPAS, both from the University of Texas at Austin). Subsequently, this simulator was improved using a fully second-order scheme, along with a total variation diminishing formulation in the mass conservation equation, validating both its results against the mentioned simulators and its order of accuracy in secondary and tertiary recovery processes.[44] Thus, it is considered that the validation was already done and reported.[41,45,46] Hence, the partial differential equations describing a compositional fluid flow in porous media are based on the momentum and mass balances.[41,47,48]

Momentum Balance. There are mainly two different approaches when modeling flow in porous media: the direct model describing the flow at a poral scale using variations of Navier−Stokes (creeping flow) equations and the continuum model which is used in a macroscopic, field-scale level, considering average properties of both fluids and rocks over a representative elementary volume (REV). The continuum model is used in this simulator to study the chemical EOR processes and involves using the Darcy equation for a multiphase flow.

$$\vec{u}^{\,j} = -\underline{\underline{K}}\frac{k_r^j}{\mu^j}\vec{\nabla}p^j \quad j = o,\ a \tag{1}$$

Mass Transport. In chemical EOR processes a multiphase, multicomponent flow is generally developed, with the processes

DOI: 10.1021/acs.energyfuels.8b02900
Energy Fuels 2018, 32, 12231−12246

therein involved characterized by the chemical and physical interactions among the components present in the fluids/rock. Therefore, advective, diffusive, and/or dispersive mixing of these components are critical processes of the mass transport and must be correctly modeled (eq 2). The molecular diffusion and hydrodynamic dispersion may be important, and they are incorporated in the flow equations by means of the diffusion/dispersion tensor (eq 3). Equations 1 and 2 are used to derive the general aqueous pressure equation of the numerical method (eq 4).

$$\frac{\partial(\phi z_i)}{\partial t} + \nabla\sum_j V_i^j \vec{u}^j - \nabla\sum_j \underline{\underline{D_i^j}}\nabla V_i^j = -\frac{\partial(\phi \mathrm{Ad}_i)}{\partial t} + q_i$$

$$i = \mathrm{p, c, w, s, pol} \tag{2}$$

$$\underline{\underline{D_i^j}} = dm_i^j \phi S^j \delta_{ij} + \|\vec{u}^j\|\left[\frac{dl^j}{\|\vec{u}^j\|^2}\begin{pmatrix}(u_x^j)^2 & u_x^j u_y^j\\ u_y^j u_x^j & (u_y^j)^2\end{pmatrix} + dt^j\begin{pmatrix}1-\frac{(u_x^j)^2}{\|\vec{u}^j\|^2} & -\frac{u_x^j u_y^j}{\|\vec{u}^j\|^2}\\ -\frac{u_y^j u_x^j}{\|\vec{u}^j\|^2} & 1-\frac{(u_y^j)^2}{\|\vec{u}^j\|^2}\end{pmatrix}\right] \tag{3}$$

$$\phi c_r \frac{\partial p^a}{\partial t} + \vec{\nabla}(\lambda \nabla p^a) = \frac{\partial}{\partial t}\left(\phi\sum_i \mathrm{Ad}_i\right) - \vec{\nabla}(\lambda^o \nabla p_c) + q_t \tag{4}$$

Nondimensionalization of the Momentum and Transport Equations. Along with the definition and discretization of the PDEs, it is important in every physical system to establish the degree of influence and dominance of the different phenomena and properties involved. In order to accomplish this, the dimensionless form of these PDEs should be derived and analyzed, which is presented in eqs 5 and 6, expressed using dimensionless groups such as the Capillary and Peclet numbers (eq 7). The dimensionless variables are represented using a breve symbol (˘).

$$\breve{\nabla}\left[\left(\frac{k_r^o}{N_{vc}^o} + \frac{k_r^a}{N_{vc}^a}\right)\breve{\nabla}\breve{p}^a\right] = \phi\frac{\partial}{\partial \breve{t}}\left(\sum_i \mathrm{Ad}_i\right) - \breve{\nabla}\left(\frac{k_r^o}{N_{vc}^o}\breve{\nabla}\breve{p}_c\right) + t_{\mathrm{ref}} q_t \tag{5}$$

$$\phi\frac{\partial z_i}{\partial \breve{t}} + \breve{\nabla}\sum_j V_i^j \breve{u}^j - \breve{\nabla}\sum_j \frac{1}{\mathrm{Pe}_i^j}\breve{\nabla}V_i^j = -\phi\frac{\partial \mathrm{Ad}_i}{\partial \breve{t}} + t_{\mathrm{ref}} q_i \tag{6}$$

$$N_{vc}^j = \frac{u_{\mathrm{ref}}^j K}{\lambda^j \sigma} \wedge \mathrm{Pe}_i^j = \frac{l_{\mathrm{ref}} u_{\mathrm{ref}}^j}{D_i^j} \tag{7}$$

The Capillary represents the relationship between viscous and capillary forces and affects the momentum equation. The surfactants aim at making these forces of a similar order so the trapped oil can be displaced. On the other hand, the Peclet number defines the relative importance of the diffusion mechanisms in the mass transport equation. Negligible diffusion coefficients render a high Peclet number ($\mathrm{Pe}_i^j \gg 1$) where then the advection dominates. With increasing diffusion coefficients, the Peclet number is low ($\mathrm{Pe}_i^j \approx 1$ or $\mathrm{Pe}_i^j < 1$), and thus, diffusion mechanisms can no longer be neglected.

PHYSICAL PROPERTIES

Chemical Component Partition. The first and most relevant part of the physical properties in a chemical EOR simulator is how the different species distribute in the phases present in the reservoir. A SP flooding can be reasonably well represented, as the surfactant EOR process, in a ternary phase diagram, wherein the chemical compound is located in the apex while the other two components, the water and oil, occupy the lower vertices. The composition of a mixture is determined by any point inside the triangle.[49−51] The numerical simulation of the model involves a two-phase, five pseudocomponent system. It is assumed in this model that the surfactant can stay both in the aqueous or oleous phases while polymer and salt remain only in the aqueous phase, independently of the kind of emulsion, Type II(−) or II(+), present in the reservoir.[13,14] Therefore, the equations needed to make the system determined are listed below.

$$\text{solubilization coefficient} = L_{\mathrm{pc}}^a = \frac{V_{\mathrm{p}}^a}{V_{\mathrm{c}}^a} \tag{8}$$

$$\text{swelling coefficient} = L_{\mathrm{wc}}^o = \frac{V_{\mathrm{w}}^o}{V_{\mathrm{c}}^o} \tag{9}$$

$$\text{partition coefficient} = k_{\mathrm{c}} = \frac{V_{\mathrm{c}}^o}{V_{\mathrm{c}}^a} \tag{10}$$

The value of k_c determines two different two-phase emulsions: Type II(−) (for $k_c < 1$) and Type II(+) systems (for $k_c > 1$). The partition coefficient depends on the composition (i.e., surfactant type) and the water characteristics, such as temperature and salinity. The partition coefficient can be modeled as a piece-wise function of the salinity in the reservoir (eq 11).[13,52]

$$k_c = \begin{cases} 10^{2(V_s^a/V_{s,\mathrm{opt}}^a - 1)} & \text{if } V_s^a > V_{s,\mathrm{opt}}^a \\ 10^{2(1 - V_s^a/V_{s,\mathrm{opt}}^a)} & \text{if } V_s^a < V_{s,\mathrm{opt}}^a \end{cases} \tag{11}$$

The other two relationships are obtained from the polymer and salt partition in the phases. These species are present only in the aqueous phase ($V_s^o = V_{\mathrm{pol}}^o = 0$). With these five relationships the system is numerically determined and all the concentrations can be calculated. Figure 4 depicts the physical model of the five-component system and its representation in ternary diagrams, such as in the surfactant flooding. In this case a simplification of the surfactant partition is used in order to calculate the phase properties.

Interfacial Tension. The interfacial tension (IFT) of the system depends on the presence and concentration of the several chemical species used during the EOR process. In surfactant flooding, this was modeled as a function of the emulsion type as well.[39,50,53−55] However, in this case an expansion of the previous model is proposed to take into account the presence of the salt. The oil−water (no chemical) IFT is dependent on the salinity. In this simulator a correlation to modify this value considering the TDS is used, as presented in eq 12.[26]

$$\sigma_{\mathrm{salt}}^{ow} = \sigma_{\mathrm{H}}^{ow} + 0.0334T\ln(1 + 4.43V_s^a) \tag{12}$$

where σ_{H}^{ow} is the IFT of the water−oil system and T is the temperature. For Type II(−) systems (oil/water emulsion):

$$\log(\sigma_c) = \log(F) + (1 - L_{\mathrm{pc}}^a)\log(\sigma^{\mathrm{H}}) + \frac{G_1}{1 + G_2}L_{\mathrm{pc}}^a \quad L_{\mathrm{pc}}^a < 1$$

$$\log(\sigma_c) = \log(F) + \frac{G_1}{1 + L_{\mathrm{pc}}^a G_2} \quad L_{\mathrm{pc}}^a \geq 1 \tag{13}$$

For Type II(+) systems (oil emulsion/water):

DOI: 10.1021/acs.energyfuels.8b02900
Energy Fuels 2018, 32, 12231−12246

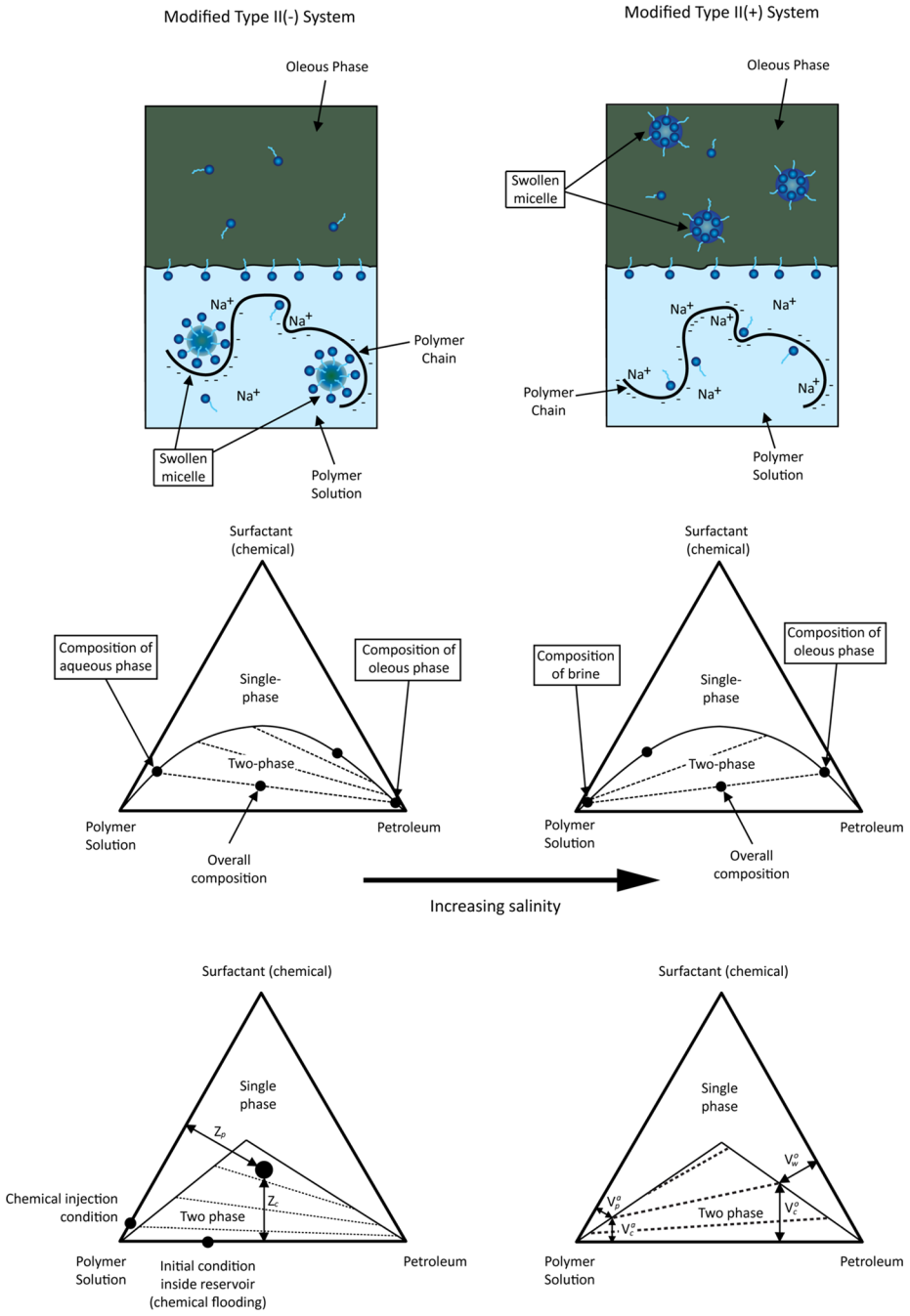

Figure 4. Ternary phase diagrams including the presence of the polymer for type II(−) (left) and II(+) (right) systems (top) and their simplified representations (bottom) (adapted from Druetta[43]).

$$\log(\sigma_c) = \log(F) + (1 - L^o_{wc})\log(\sigma^H) + \frac{G_1}{1 + G_2}L^o_{wc} \quad L^o_{wc} < 1$$

$$\log(\sigma_c) = \log(F) + \frac{G_1}{1 + L^o_{wc}G_2} \quad L^o_{wc} \geq 1 \tag{14}$$

Constants G_1 and G_2 are input parameters, and the term F is obtained according to the following equation.[52]

$$F = \frac{1 - e^{-\sqrt{\sum_{i=p,w,c}(V_i^o - V_i^a)^2}}}{1 - e^{-\sqrt{2}}} \tag{15}$$

In chemical recovery processes, the presence of the surfactant causes the decrease of IFT, allowing the mobilization of oil trapped in the reservoir, so it can be inferred that the residual saturations depend on the IFT. The IFT of the water−oil system (no surfactant present) is considered constant throughout the simulation. The influence of the polymer, explained previously, is taken into account as the last part of the IFT calculation procedure, which represents a novel approach from previous SP simulators. The values obtained due the presence of the surfactant are then modified accordingly.[17,18,56−59]

$$\sigma = \sigma_c\left(1 + \frac{\mathrm{IFTpol}K V^a_{pol}}{1 + e^{k_c Z_c / Z_c^{crit}}}\right)^{\mathrm{IFTpol}n} \tag{16}$$

$$\mathrm{IFTpol}K = \mathrm{IFTpol}K_{max}(1 - e^{-C_{pol}V^a_{pol}}) \tag{17}$$

DOI: 10.1021/acs.energyfuels.8b02900
Energy Fuels 2018, 32, 12231−12246

The terms IFTpolK_{max}, Z_c^{crit}, IFTpol$n$, and C_{pol} are input parameters considering the influence of the surfactant and polymer in the water−oil IFT. The parameter IFTpol$K$ follows an exponential law allowing the polymer influence to be negligible as its concentration goes to zero. In the propose formulation the partition coefficient is included as a term affecting the influence of the polymer, since it is assumed that the polymer's influence on the IFT becomes negligible as the partition coefficient increases and the surfactant tends to be present only in the oleous phase (Figure 5). This formula affects the IFT only when

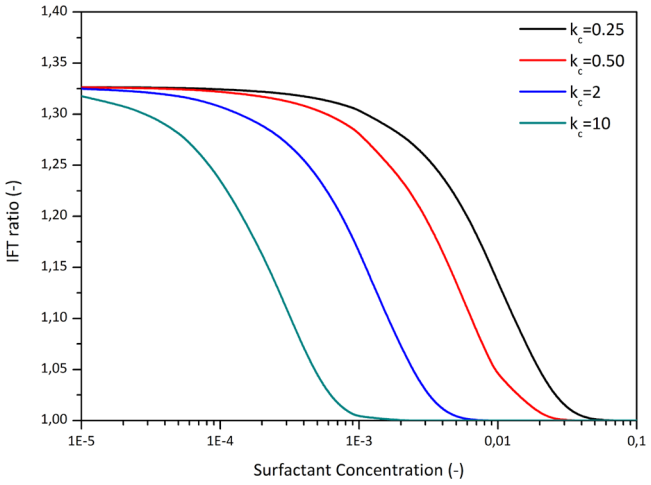

Figure 5. Interfacial tension ratio (IFT^{pol}/IFT) considering the influence of the polymer, the partition coefficient, and the surfactant concentration.

the surfactant is present in the representative elementary volume (REV). Below a certain concentration, the influence of the polymer in the IFT is not considered. Finally, in this study it is not included in the scope the possible influence of hydrophobically modified polymers in the interfacial tension. The joint presence of these and surfactants may affect the behavior of the system, modifying Figure 1.

Residual Saturation. Residual saturations play an important role in oil recovery processes. They establish a certain limit to how much oil can be mobilized during the process. If such saturations can be reduced, this will increase the efficiency of the whole process. As explained in the previous section, they depend on the IFT in the water−oil two-phase system. The presence of the surfactant can modify the residuals saturations in the porous medium. This relationship is ruled by a dimensionless group, the capillary number, defined by the following equation:

$$N_{vc} = \frac{uK}{\lambda\sigma} \tag{18}$$

The functionality between the capillary number and the residual saturation for both phases is described by the following model:[39]

$$\frac{S^{jr}}{S^{jrH}} = \begin{cases} 1 & \text{if} \quad N_{vc} < 10^{(1/T_1^j)-T_2^j} \\ T_1^j[\log(N_{vc}) + T_2^j] & \text{if} \quad 10^{(1/T_1^j)-T_2^j} \le N_{vc} \le 10^{-T_2^j} \\ 0 & \text{if} \quad N_{vc} > 10^{-T_2^j} \end{cases} \tag{19}$$

The piecewise function is defined by constant parameters which depend on the fluids and the porous medium being injected. The relationship between the residual saturation after chemical and waterflooding processes is known as the normalized residual saturation of phase j. The form of eq 19 for both phases determines what is known as capillary desaturation curves (Figure 6).

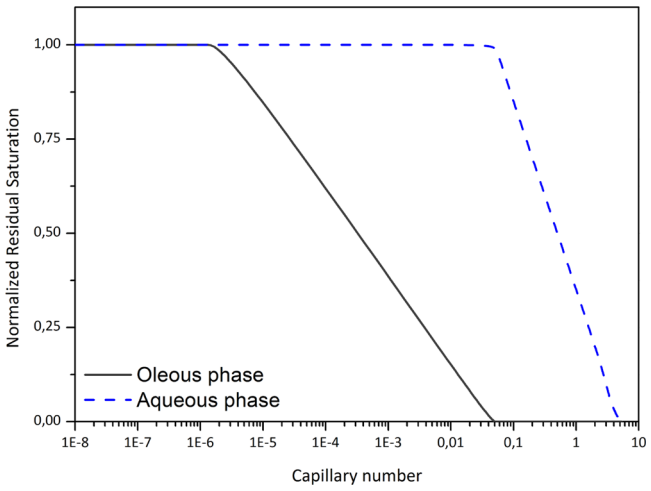

Figure 6. Capillary desaturation curves for nonwetting (oleous) and wetting (aqueous) phases used for this simulation.

At low capillary numbers, the behavior is similar to a process of waterflooding and the normalized residual saturation is not decreased. As the IFT decreases and/or the viscosity increases, the capillary number raises to values higher than those of the secondary recovery. It is for this reason that in areas of high speeds (i.e., nearby the wells) oil saturation values lower than those of waterflooding can be achieved. The aqueous phase usually requires higher values of N_{vc} to achieve a full desaturation.[14]

Relative Permeabilities. Relative permeabilities influence Darcy's equation on the phase velocities and, therefore, the efficiency of oil recovery. They depend on the residual saturations which were calculated in the previous section. The model used to calculate the relative permeabilities is taken from Camilleri,[60,61] which is used for most chemical flooding processes. Knowing beforehand the phase saturations, the relative permeabilities are calculated according to the following formula:

$$k_r^j = k_r^{j0}\left(\frac{S^j - S^{jr}}{1 - S^{jr} - S^{j'r}}\right)^{e^j} \quad j = o, a; \; j \neq j' \tag{20}$$

where k_r^{j0} and e^j represent the end point and the curvature of the function $k_r^j(S^j)$. These values are calculated by the following equations:

$$k_r^{j0} = k_r^{j0H} + (1 - k_r^{j0H})\left(1 - \frac{S^{j'r}}{S^{j'rH}}\right) \quad j = o, a; \; j \neq j' \tag{21}$$

$$e^j = e^{jH} + (1 - e^{jH})\left(1 - \frac{S^{j'r}}{S^{j'rH}}\right) \quad j = o, a; \; j \neq j' \tag{22}$$

where k_r^{j0H} and e^{jH} are the end point values of curvature and relative permeability function system for water−oil without the presence of chemical agents, respectively.

Phase Viscosities. The effect of the polymer is to increase the viscosity of the sweeping phase (water), whereas it has little or negligible effect on the microemulsion and oleous phases, unless the former is the water-rich phase. The surfactant, on the

DOI: 10.1021/acs.energyfuels.8b02900
Energy Fuels 2018, 32, 12231−12246

other hand, has two effects on the polymer viscosity according to Sheng:[13] it brings cations such as Na^+, reducing the solution viscosity because of electrostatic interactions with the polymer molecules; and when the surfactant is added, aggregates might be formed and the solution viscosity is increased. All in all, surfactant does not significantly affect the rheology of the aqueous phase. In this simulator, the viscosity of each phase depends on its composition as a function of the volumetric concentration of each component. Due to the influence on the viscosity from all the components, a stepwise approach was adopted in the viscosity calculations. First, the influence of the salt on the pure water/brine viscosity is calculated:[50,55]

$$\mu_{\text{brine}} = \mu^a(1 + A_{\text{sal}}V_s^a + B_{\text{sal}}V_s^{a^2}) \tag{23}$$

where A_{sal} and B_{sal} are constants based on rheology experiments. Second, the influence of the other two components, petroleum and surfactant, is evaluated on the viscosity of both phases. For the oil phase, it was assumed a Newtonian behavior for pure oil. It is considered that light and medium oil cuts exhibit Newtonian behavior while heavy oil might present a slight shear-thinning rheology.[62]

$$\mu^j = V_w^j\mu^{a\text{H}}e^{\alpha 1(V_p^j+V_c^j)} + V_p^j\mu^{o\text{H}}e^{\alpha 1(V_w^j+V_c^j)} + V_c^j\alpha_3 e^{\alpha 2(V_w^j+V_o^j)} \quad j = o, a \tag{24}$$

where α_k are constants and $\mu^{a\text{H}}$ and $\mu^{o\text{H}}$ are values of viscosity in the water−oil system without surfactant. Finally, the influence of the polymer on the aqueous phase is considered:

$$\mu_{\text{UVM}} = \mu_{\text{ST}} + \mu_{\text{ELAS}} \tag{25}$$

$$\mu_{\text{ST}} = \mu_{0\text{sr}} + (\mu_w - \mu_{0\text{sr}})\left[1 + \left(\frac{\dot{\gamma}}{\tau_r}\right)^2\right]^{(n-1/2)} \tag{26}$$

$$\mu_{\text{ELAS}} = \mu_{\text{max}}[1 - e^{-(\lambda_2\tau_2\dot{\gamma})^{n_2-1}}] \tag{27}$$

$$\mu_{0\text{sr}} = \mu_w[1 + (\text{AP}_1V_c^a + \text{AP}_2V_c^{a^2} + \text{AP}_3V_c^{a^3})C_{\text{SEP}}^{Sp}] \tag{28}$$

where AP_1, AP_2, and AP_3 are input parameters which can be obtained from laboratory experiments and in the model are expressed as a function of the intrinsic viscosity and the polymer's molecular weight. The term C_{SEP}, known as the effective salinity for the polymer component, cannot be longer considered constant and is calculated according to the following equation (provided the salt is considered as the fifth component in the reservoir):

$$C_{\text{SEP}} = \frac{V_s^a + (\beta_{\text{pol}} - 1)C_{\text{div}}^a}{V_w^a} \tag{29}$$

where C_{DIV}^a is the concentration of divalent cations in the water phase, which is assumed to be negligible. The constant β_{pol} is obtained from laboratory measurements.[52]

Adsorption. The adsorption process in porous media takes place, and a layer of the EOR chemical components form onto the surface of the formation rock. This phenomenon causes a substantial loss of the chemicals in the porous media, affecting the saturations and concentrations in eq 2, rendering the process economically unfeasible. The adsorption rate is dependent on the type of chemical, the characteristics of the rock, and the type of electrolytes present in the phases. Due to the IAPV phenomenon, the polymer flows in front of the surfactant slug and therefore is "sacrificed" during the flooding process.[13] Thus, the formation will be covered by polymer molecules, and fewer sites will be available for the surfactant adsorption to occur, which is known as competitive adsorption. In order to consider this, a formulation was introduced in which the surfactant adsorption is a function of adsorbed polymer concentration, and vice versa.

$$F_{\text{SP}} = 1 - \frac{\text{Ad}_{\text{pol}}}{\text{Ad}_{\text{max,pol}}}F_{\text{ads}} \wedge F_{\text{SP}}^{\text{pol}} = 1 - \frac{\text{Ad}_c}{\text{Ad}_{\text{max,c}}}F_{\text{ads}}^{\text{pol}} \tag{30}$$

where $\text{Ad}_{\text{pol,c}}$ is the amount of adsorbed polymer/surfactant and $\text{Ad}_{\text{max,pol,c}}$ is the asymptotic value of the Langmuir model. The parameters F_{ads} and $F_{\text{ads}}^{\text{pol}}$ can be adjusted based on the pair of chemicals used to consider the competitive process. Thus, the adsorption of both chemical species is as follows:

$$\text{Ad}_{\text{c,pol}} = \min\left[(Z_{\text{c,pol}} + \text{Ad}_{\text{c,pol}}), \frac{F_{\text{SP}}^{(\text{pol})}a_{1,\text{c,pol}}Z_{\text{c,pol}}}{1 + a_{2,\text{c,pol}}Z_{\text{c,pol}}}\right] \tag{31}$$

Due to the coefficient $F_{\text{SP}}^{(\text{pol})}$, the maximum value in the surfactant adsorption process is reduced ($F_{\text{SP}}^{(\text{pol})} \neq 0 \wedge \text{Ad}_{\text{c,pol}} \neq 0$) or unchanged ($F_{\text{SP}}^{(\text{pol})} = 0 \vee \text{Ad}_{\text{c,pol}} = 0$). Conversely, if the surfactant slug is injected ahead of the polymer, the rock will be covered by the former, reducing the polymer adsorption. The parameter $a_{1,\text{pol,c}}$ is function of the TDS present in the reservoir.

$$a_{1,\text{c}} = (a_{11,\text{c}} + a_{12,\text{c}}C_{\text{SE}})$$
$$a_{1,\text{pol}} = (a_{11,\text{pol}} + a_{12,\text{pol}}C_{\text{SEP}}) \tag{32}$$

where C_{SE} is the effective salinity for the surfactant component, taking into account the concentration of dissolved salts in the aqueous phase, along with thermal effects and the fraction of total divalent cations.

$$C_{\text{SE}} = V_s^a\frac{1}{1 - \beta_{\text{div}}f_{\text{div}}}\frac{1}{1 + \beta_{\text{temp}}(T - T_{\text{ref}})} \tag{33}$$

The parameter C_{SEP} is the effective salinity for the polymer and cannot be considered constant. This is also a function of the concentration of salts in the porous medium.

$$C_{\text{SEP}} = \frac{V_s^a + (\beta_{\text{pol}} - 1)C_{\text{div}}^a}{V_w^a} \tag{34}$$

where C_{DIV}^a is the concentration of divalent cations in the water phase, assumed in this model to be negligible. The constant β_{pol} is usually obtained from laboratory measurements.

RESULTS AND DISCUSSION

Introduction. The aim of the simulations in this paper is to find the optimal injection scheme as well as to determine the most appropriate moment to start with the EOR process. Therefore, four different injection schemes were tested: polymer injected in the first place, followed by a surfactant slug (separated/overlapped), and vice versa. According to the literature, a polymer preflush improves the vertical conformance of the surfactant solution and the final recovery factor. Moreover, when polymer is injected before surfactant, the SPI phenomenon seems to be relieved.[13] With respect to the injection scheme, Sheng[13] reported that according to experimental results the best outcomes were obtained when the chemicals were injected separately and not as a single slug. Regarding the order of injection, the same study concluded that injecting the polymer in the first term yielded the best results, which was also corroborated by Liu.[28]

In order to meet the objectives, a series of SP simulations are presented in reservoirs with similar physical properties, but

DOI: 10.1021/acs.energyfuels.8b02900
Energy Fuels 2018, 32, 12231−12246

which have been exploited in different production conditions. In order to set benchmark values, standard polymer and surfactant flooding processes are simulated and then compared with the four different injection methods mentioned previously. Subsequently, and using the SP scheme that yielded the best results, the influence of the starting point of the EOR process is discussed. To that end, a series of waterflooding processes were simulated, finishing at different values of fractional flow in the producing well, e.g., 0.85, 0.90, 0.95, and 0.99. These secondary recoveries are followed by the same SP injection scheme, with comparison and discussion of the results and the strategies to be used in SP flooding processes.

Data. In order to study the combined EOR flooding, several major parameters of the geometrical dimensions, simulation conditions, and physical properties are established beforehand in order to represent a standard low-viscosity oil field after primary recovery, which will be the target of the combined CEOR operations (Tables 1 and 2).

Table 1. Geometrical and Initial Reservoir Parameters

Geometrical Data of the Reservoir					
length (axis X)	500 m	length (axis Y)	500 m	reservoir thickness	5 m
n_x elements	25	n_y elements	25		
Rock Properties					
porosity	0.25	k_{xx}	200 mD	k_{yy}	200 mD
Initial Conditions					
S_o	0.70	S_o^r (EOR)	0.35	$S_a^{rH} = S_o^{rH}$	0.15
Simulation Data					
total time	3000 d	surf. inj. time	100 d	z_{clN}	0.1
		pol. inj. time	100 d	z_{polN}	0.025
Physical Data of the Phases					
μ^{aH}	1 cP	μ^{oH}	10 cP	oil density	850 kg/m^3
water density	1020 kg/m^3	IFT	50 mN/m		

Table 2. Operational Conditions for the Wells

Physical Data					
no. of wells	2	well radius	0.25 m	skin factor	0
Operating Conditions					
total flow rate	1400 STB/day	bottomhole pressure	55160 kPa		

Influence of the Injection Scheme. The first part of the analysis is the study of the influence of the injection scheme during a two-phase, four-component SP flooding. Four different schemes were developed to study the influence of chemical sequence, with the option of injection separately or with an overlap between slugs of polymer and surfactant. The results of these simulations are presented in Table 3 and Figures 7 and 8, together with the reference cases that were mentioned above.

As expected, the SP process presented in all its variants an increase in the recovered oil with respect to the processes of waterflooding and traditional chemical EOR methods. It is noteworthy that even though there was an increase in the recovery factor, there was also an increment in the associated costs, which were not taken into account in this simulator. The profitability of EOR operations depends on several factors which are out of the scope of this paper. Considering only the SP processes, it is observed that the best results for this type of reservoir were obtained when the polymer was injected first. This increases the efficiency of the first sweeping front, and then the residual oil is displaced by the surfactant along with the water bank toward the producing well. Regarding the question of whether a separate injection or an overlap is better, the results show that, although the difference is small, the optimal sweep scheme is obtained when both chemical slugs present a slight overlapping. It is also noteworthy from Table 3 that the recovery efficiency of a standard surfactant flood is strongly dependent on the mobility ratio, and better results are achieved with similar or even smaller polymer slugs due to lower mobility ratios.

As mentioned above, these conclusions were obtained for a reservoir and crude oil of the characteristics listed in Tables 1 and 2. Further simulations are deemed necessary for other types of oil and reservoirs, in which the factors that affect the sweeping efficiency could be significantly altered (e.g., the mobility ratio).

Table 4 and Figures 7 and 8 show the trend explained above. The combined process increased the recovery and oil flow and also decreased the operational time to reach the economic limits of fractional flow in the producing well. The pressure drop values (Figure 7, right) do not show significant differences between the SP process and the polymer flooding taken as reference, since the influence of surfactant on the rheological properties is not relevant. However, there is a notorious difference between the mentioned processes and the water- and surfactant-flooding techniques, in which the value of the mobility ratio is much greater. Moreover, Figure 8 (right) shows what has been discussed during the introduction; due to the IAPV phenomenon, the polymer moves faster than the surfactant molecules, which is reflected in the chemical breakthrough times and the concentration profiles as a function of time.

Figures 9, 10, and 11 show the oil saturation profiles for the different SP flooding cases. Even though the areal sweeping efficiency is comparable in the different injection schemes, the surfactant being injected after the polymer allowed total desaturation of a bigger region of the reservoir, even in these simulations using a surfactant with a low partition coefficient, to form a Type II(−) emulsion. The pressure profile in Figure 12 complements the behavior observed in Figure 7 (right). The pressure drop in these cases is significantly higher than those obtained in standard flooding schemes. This is due to several factors, namely, increased flow rate and different constants used in the polymer viscosifying properties. This notoriously modified the pressure gradient in the areas near injection and producing wells.

In addition to Figure 7 (right), at the end of the process there was no difference between water and surfactant flooding because, in the case of surfactant, the smaller size of its molecules does not cause the phenomenon of disproportionate

Table 3. Results of the Recovery Process for Different SP Flooding Schemes and the Reference Cases

case	oil recovered		case	oil recovered	
	m^3	% OOIP		m^3	% OOIP
reference polymer	90691	48.4	polymer + surfactant (overlapped)	100581	53.6
reference surfactant	76060	40.6	polymer + surfactant (separated)	97017	51.7
reference surfactant ($t_{inj} = 2 \times t_{surf}$)	78990	42.1	surfactant + polymer (overlapped)	97769	52.1
reference surfactant ($c_{inj} = 2 \times c_{surf}$)	80580	43.0	surfactant + polymer (separated)	91687	48.9

DOI: 10.1021/acs.energyfuels.8b02900
Energy Fuels 2018, 32, 12231−12246

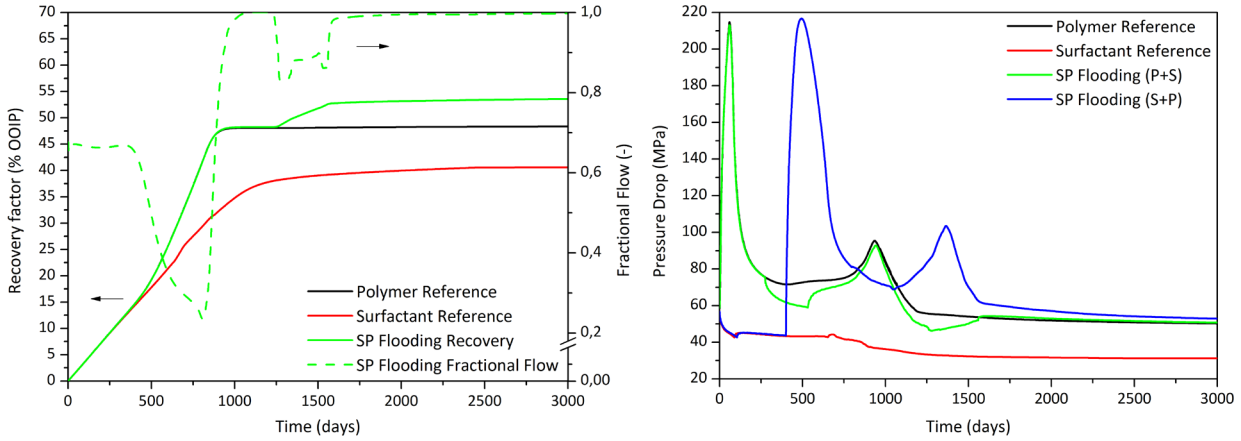

Figure 7. Oil recovery, fractional flow (left), and pressure drop (right) as a function of time for the reference cases and different SP schemes.

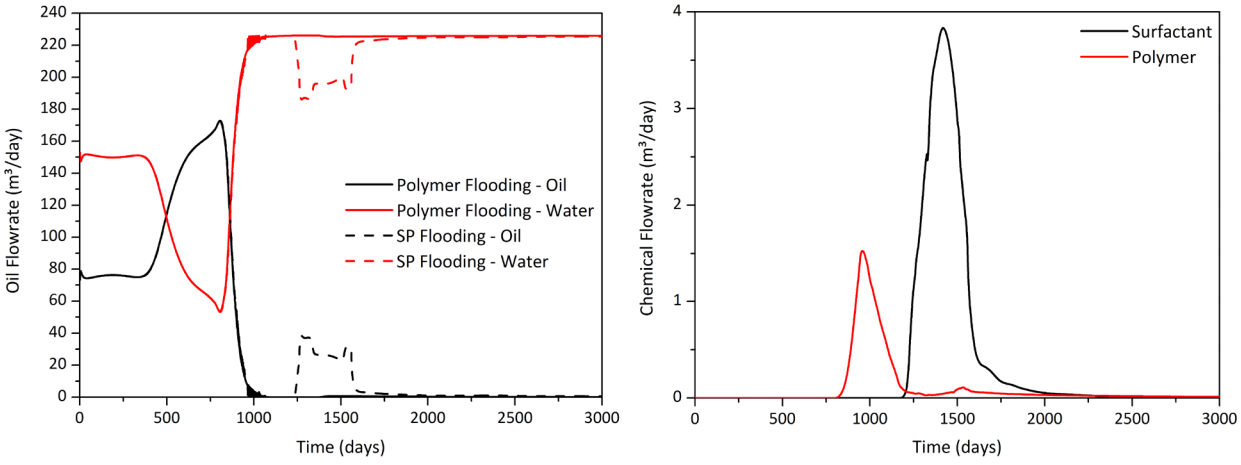

Figure 8. Water and oil flow rates (left) and chemical flow rates (right) as a function of time for the optimum SP scheme and the reference polymer flooding.

Table 4. Influence of the Water Slug Size between Chemical Injection Periods

case	time gap	oil recovered		case	time gap	oil recovered	
	days	m^3	% OOIP		days	m^3	% OOIP
pol. + surf.	175	100581	53.6	surf. + pol.	175	97769	52.1
pol. + surf.	325	98847	52.7	surf. + pol.	325	93161	49.7
pol. + surf.	425	97017	51.7	surf. + pol.	425	91687	48.9
pol. + surf.	525	94827	50.6	surf. + pol.	525	90912	48.5

permeability reduction (DPR). This is present in the SP flooding since, when no more chemical species are present in the reservoir, the final condition of pressure drop is higher than the water and surfactant flooding since the DPR irreversibly affected the relative water permeability (Figures 13 and 14).

The chemical species also present a distinctive profile, shown in Figures 15, 16, and 17. The two slugs propagate in a similar way as a 2D wave. However, in this case it the difference in the wave propagation speed is clear and is mainly due to two factors, the DPR, which causes the polymer to travel faster than the small surfactant molecules, and the influence of the phase speed, since polymer is only in water and the surfactant is present in both aqueous and oleous phases due to the phase partition model. In Figure 17 (right) the contribution of the polymer to the aqueous phase viscosity is visible. Moreover, the influence of the surfactant in the latter is slightly visible in the center of the domain. An important factor of the polymer and surfactant combined flooding is that the polymer slug limits the propagation of the surfactant, which increases its average cell concentration (in the surfactant slug region) and, therefore, its efficiency in the oil recovery process (Figure 10).

It was assumed during these simulations that the influence of the surfactant on the viscosity is practically negligible. However, in the case of polymeric surfactant flooding, this influence may no longer be neglected since the size of these surfactant molecules is big enough to affect the rheological properties of the aqueous phase and, to a lesser extent, the oleous phase viscosity. This should be a topic of future research in order to understand the synergy of these amphiphiles with polymer molecules. With respect to the IFT, the influence of the chemical species is exactly the opposite; the polymer plays no significant role in the IFT modification, while the surfactant is responsible for lowering the interfacial energy of the two-phase system.

We continue analyzing the influence of the starting point for the EOR process in this study. The best results are achieved when the EOR process starts as soon as possible, both in terms of oil recovered and in the exploitation time. With this purpose, a series of injection strategies will be compared, comprising a reference polymer case, along with the optimum SP scheme, and four coupled water and SP flooding situations. These four secondary processes were interrupted when the fractional flows at the producing well were 0.85, 0.90, 0.95, and 0.99. The results

DOI: 10.1021/acs.energyfuels.8b02900
Energy Fuels 2018, 32, 12231−12246

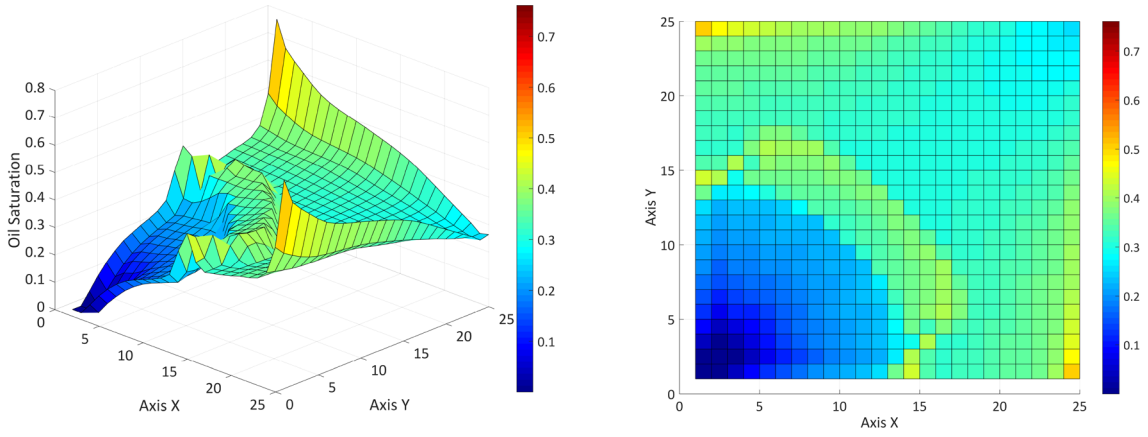

Figure 9. Oil saturation after 1000 days in a polymer + surfactant (separated) SP flooding.

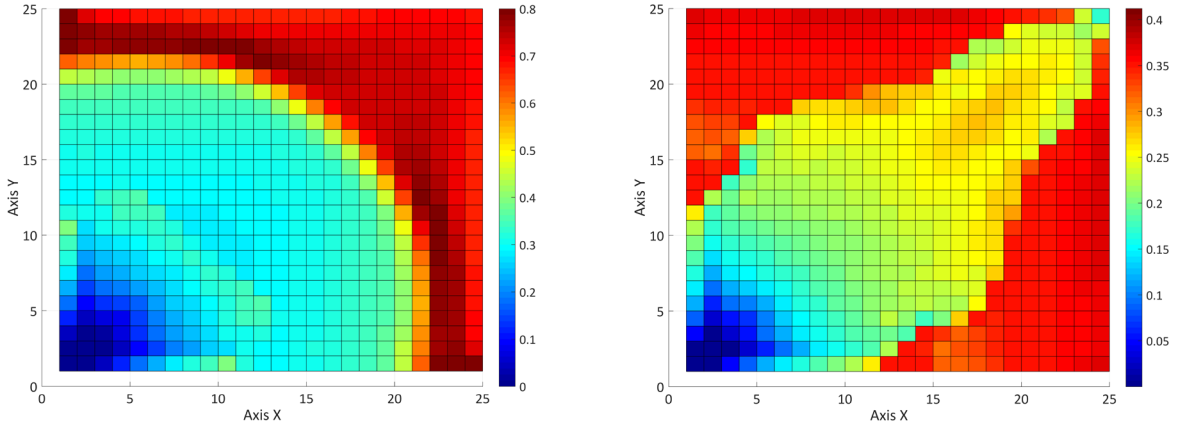

Figure 10. Oil saturation in a polymer + surfactant overlapped SP scheme after 500 days (left) and 3000 days (right). See the Supporting Information for the interactive 3D images of the simulations.

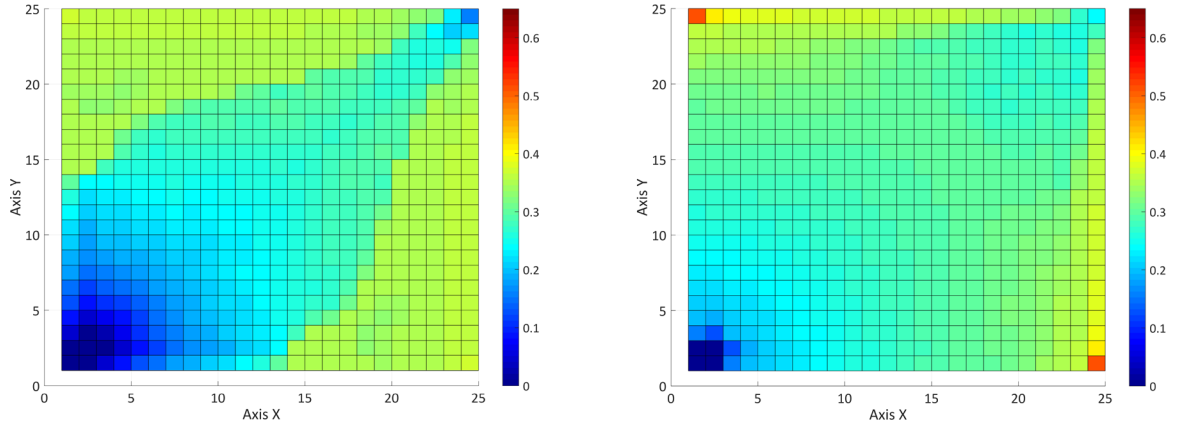

Figure 11. Oil saturation after 3000 days in a polymer + surfactant separated (left) and a surfactant + polymer separated (right) SP scheme.

for the reference case (SP without waterflooding) and the proposed cases are shown in Table 5 and in Figures 18 and 19.

These results confirm the conclusions from the literature: the earlier an EOR process begins, the better the results. This is evident when the two extreme cases are compared, focusing especially on the time spent to achieve the same oil recovery. When the SP process starts after waterflooding up to a fractional flow of 0.99, the time spent is 2.17 times longer than if the process had started with a fractional flow of 0.85. The economic benefit of this strategy is evident, although it is not reflected in the numerical simulation. However, the reasons why an EOR process should not be started immediately after the primary recovery have already been discussed, so it is advisible to perform the waterflooding up to fractional flow values lower than 0.85 while simultaneously allowing a sufficient operating time in order to be able to determine more accurately all the uncertainties associated with the reservoir.[42] The results of these secondary and tertiary recovery simulations are shown in Figures 20, 21, and 22.

The polymer slug is not affected by the initial oil saturation, although the surfactant is, due to the partition coefficient between the phases. With respect to the oil sweeping efficiency,

DOI: 10.1021/acs.energyfuels.8b02900
Energy Fuels 2018, 32, 12231−12246

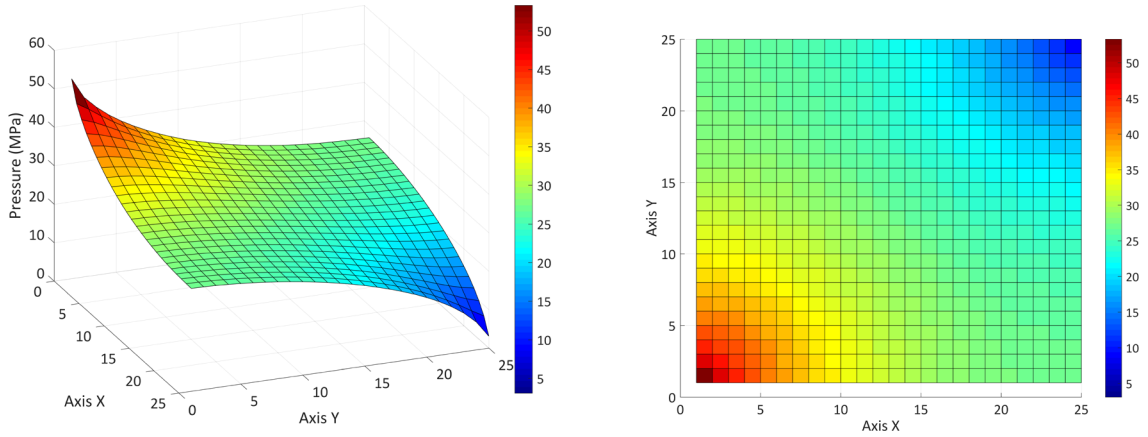

Figure 12. Pressure profile after 3000 days in a polymer + surfactant (separated) SP flooding schemes.

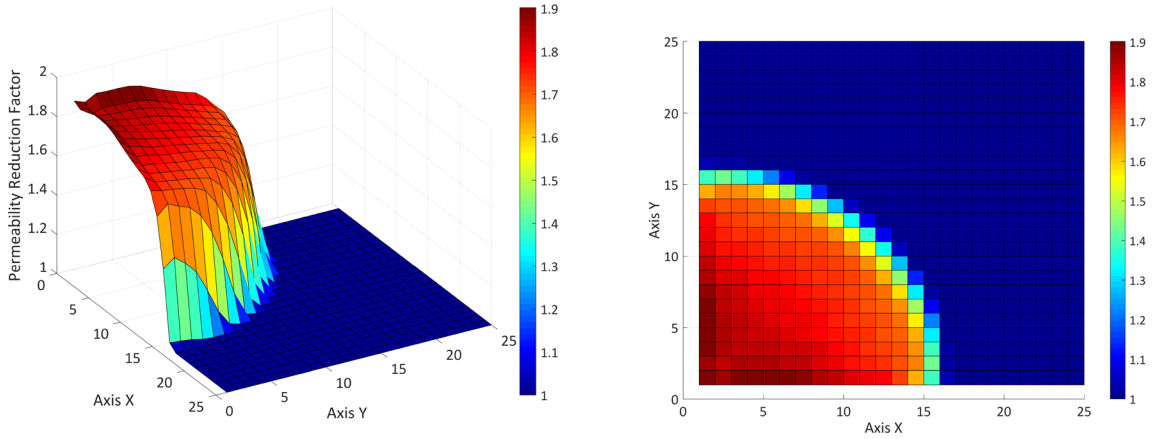

Figure 13. Disproportionate permeability reduction of the aqueous phase after 250 days in the optimum SP flooding scheme.

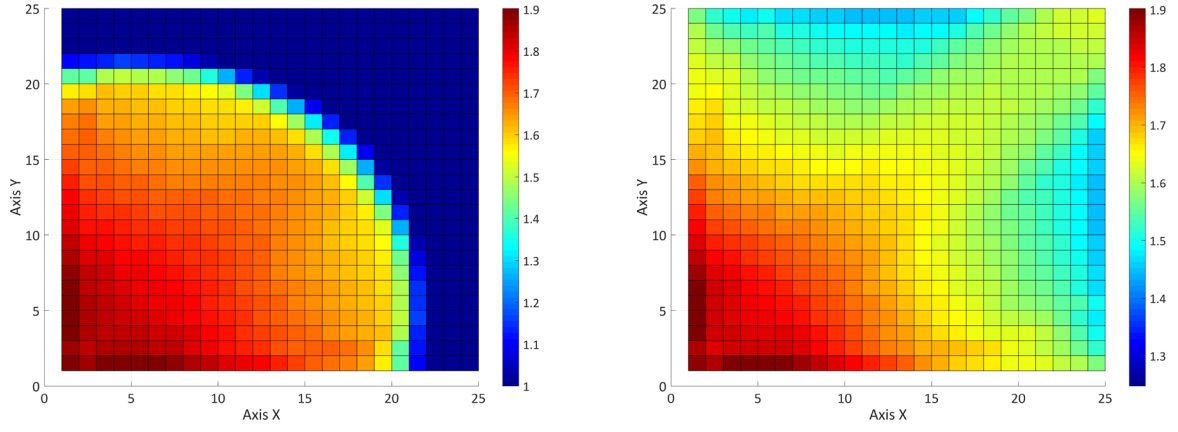

Figure 14. Disproportionate permeability reduction of the aqueous phase after 500 days (left) and 3000 days (right) for the optimum SP flooding.

it is observed that though the mobility ratio is the same in all cases, the efficiency of the displacing process changes due to the lower amount of oil that can be displaced. This is then reflected in the oil recovery factor and their exploitation times (Figure 18). As a conclusion of this analysis, the results confirmed the previous hypothesis for standard EOR cases and what is reported in the literature. Combined chemical EOR flooding shows a great potential in reservoirs with low/medium oil viscosity since it takes advantages of both chemical species and uses their synergy to increase the sweeping efficiency. This EOR process should be started as early as possible in the reservoir, but considering that the associated costs are significantly higher than those from waterflooding or secondary recovery, all the uncertainties from the oil field should be properly assessed before starting the tertiary recovery operations.[13−15,42] Moreover, it is considered that the use of polymeric surfactants will also represent a breakthrough in chemical EOR processes, and future research on this topic is advised.

All in all, the novelty of this combined EOR simulator consisted of expanding the previous models dealing with standard polymer and surfactant flooding.[43] This simulator then combines a complete degradation model for polymers, including

DOI: 10.1021/acs.energyfuels.8b02900
Energy Fuels 2018, 32, 12231−12246

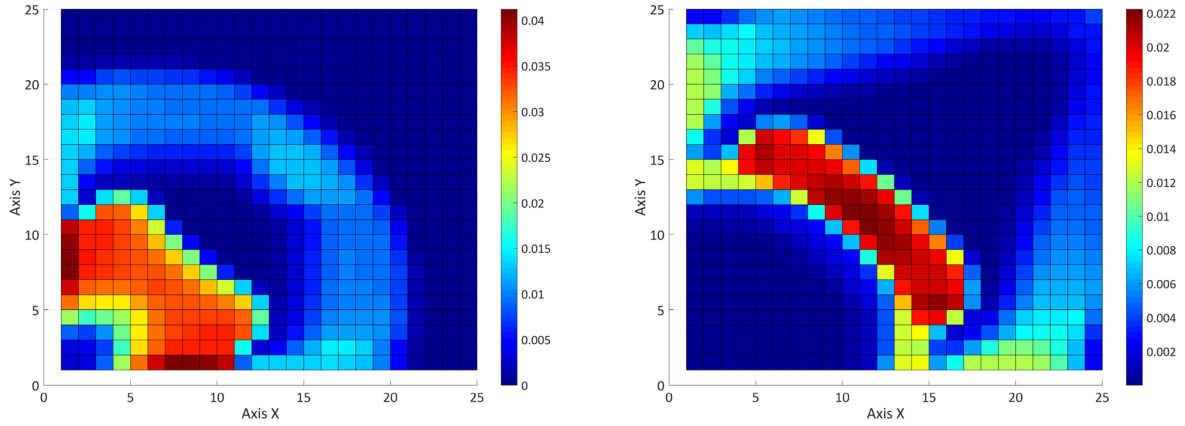

Figure 15. Combined chemical slugs in a polymer + surfactant flooding scheme after 500 days (overlapped, left) and 1000 days (separated, right).

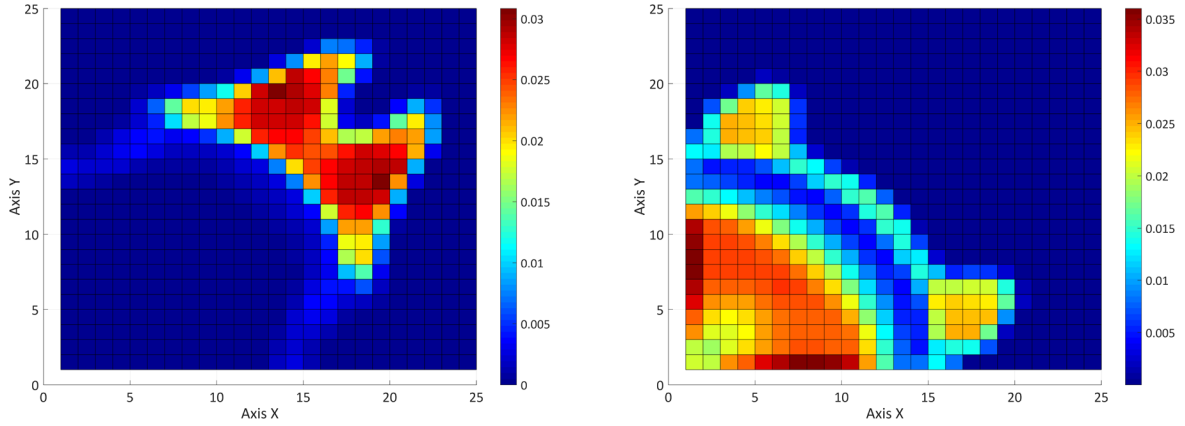

Figure 16. Surfactant profile after 1000 days in a polymer + surfactant SP scheme (overlapped, left) and combined chemical slugs after 500 days in a surfactant + polymer SP scheme (overlapped, right).

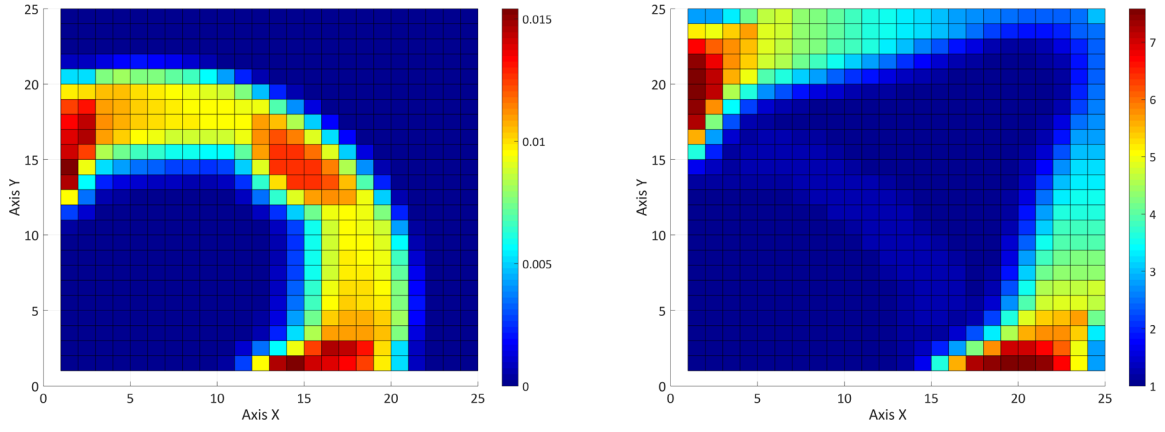

Figure 17. Polymer profile after 500 days (left) and viscosity (in mPa·s) after 1000 days (right) in a polymer + surfactant (separated) flooding scheme.

Table 5. Oil Recovery Factors for Different Water Flooding + SP Flooding, When the Critical Fractional Flow Is Modified

case	oil recovered		case	oil recovered	
	m^3	% OOIP		m^3	% OOIP
reference polymer	90691	48.4	water flooding + SP flooding (fractional flow = 0.90)	97897	52.2
reference SP flooding	100581	53.6	water flooding + SP flooding (fractional flow = 0.95)	97899	52.2
water flooding + SP flooding (fractional flow = 0.85)	97978	52.3	water flooding + SP flooding (fractional flow = 0.99)	97363	51.9

the influence of viscoelastic effects in the residual oil saturation and the phase behavior model used for surfactants based on the literature.[54,55] The next part of the study consists on adding a fifth component, the salt dissolved in the aqueous phase, and studying its influence on the combined EOR process, especially on the adsorption and viscosifying properties.

DOI: 10.1021/acs.energyfuels.8b02900
Energy Fuels 2018, 32, 12231−12246

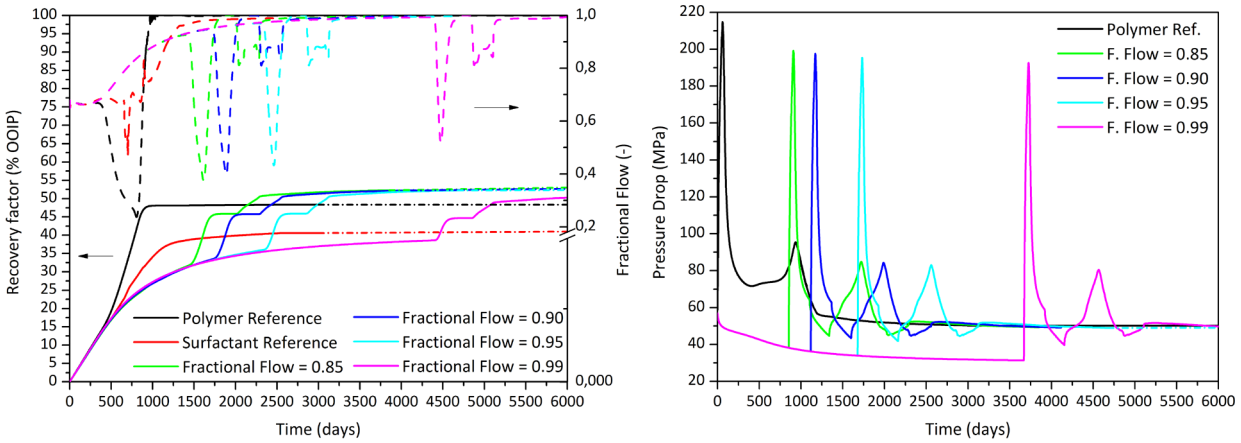

Figure 18. Oil recovery, fractional flow (left), and pressure drop (right) as a function of time for the reference cases and different water + SP schemes.

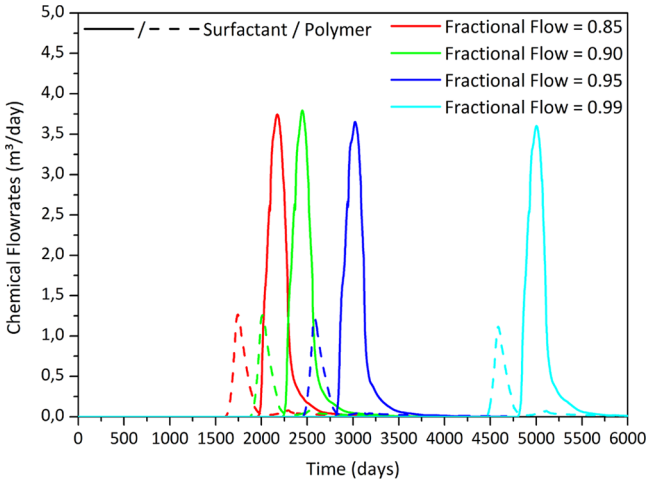

Figure 19. Chemical flow rates as a function of time for the different water + SP schemes.

CONCLUSIONS

The objective of this paper was to present a new simulator to evaluate a combined process of chemical EOR flooding using surfactant and polymers. The system evaluates the performance of the chemicals in a 2D field, considering a two-phase system with five pseudocomponents. The model is based on previous standard EOR processes, namely, polymer and surfactant flooding, adding the SPI in order to evaluate the interaction between both chemicals. The physical model was described by a system of nonlinear differential equations, which are solved by the finite difference method, elaborating an algorithm which was implemented in MathWorks MATLAB. The simulations were focused on analyzing the process and injection sequences and determine the optimum timing for the start of EOR operations. The efficiency of the injection scheme was studied using four possible schemes. The best results were obtained when the polymer was first injected followed by surfactant, with a small overlapping between the slug, which coincides with previously published results.

The SPI have not shown a noticeable effect in both the IFT and the viscosity. However, it is considered necessary to develop further mathematical models in order to simulate the synergy of hydrophobically modified polymers with surfactants, since their interactions might lead to major variations in these parameters. The second point was to analyze the optimum moment to start EOR operations. The results of this paper coincide with what was previously reported by other authors; EOR processes should be initiated as soon as possible. However, there are a number of limitations, both technical and economic, that make this difficult to carry out. Therefore, it is recommended to continue with the recovery schemes used nowadays; that is, to perform a previous waterflooding before the EOR flooding. However, the results have shown that the waterflooding should be as short as possible in order to reduce the total operational life and increase the oil recovered. This secondary recovery operating period should be used to assess all the uncertainties of the physical system and to

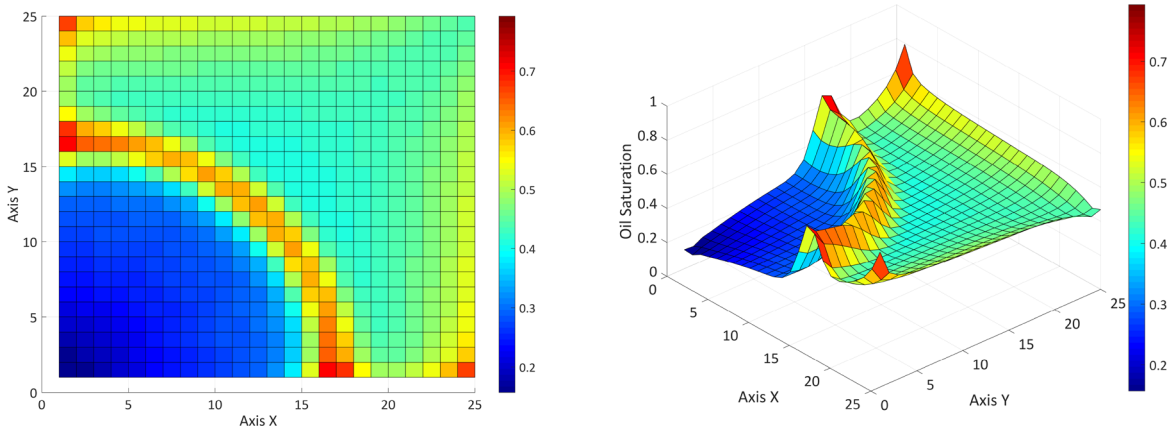

Figure 20. Oil saturation profile after 250 days of a SP flooding starting after a critical fractional flow of $f_f = 0.85$.

DOI: 10.1021/acs.energyfuels.8b02900
Energy Fuels 2018, 32, 12231−12246

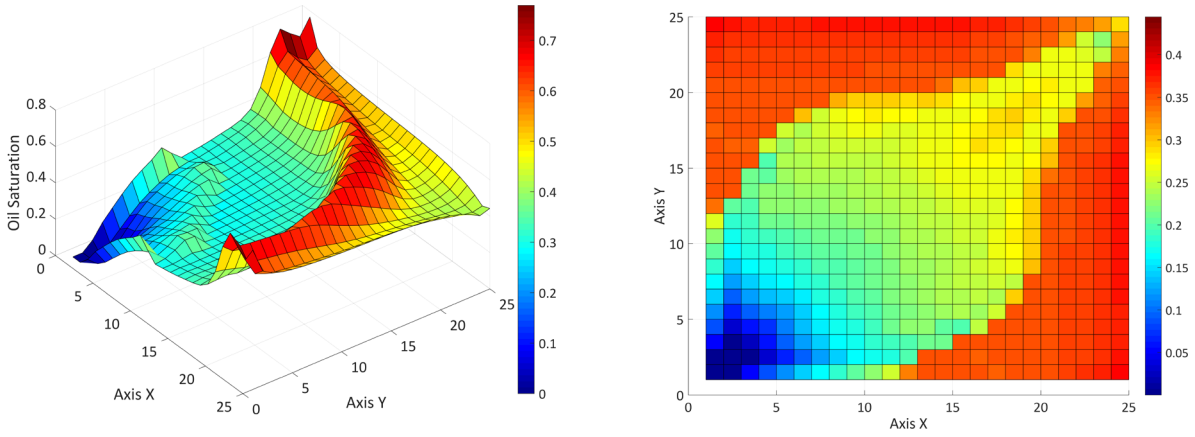

Figure 21. Oil saturation profile after 500 (left) and 3000 days (right) of SP flooding starting after a critical fractional flow of $f_f = 0.85$. See the Supporting Information for the interactive 3D images of the simulations.

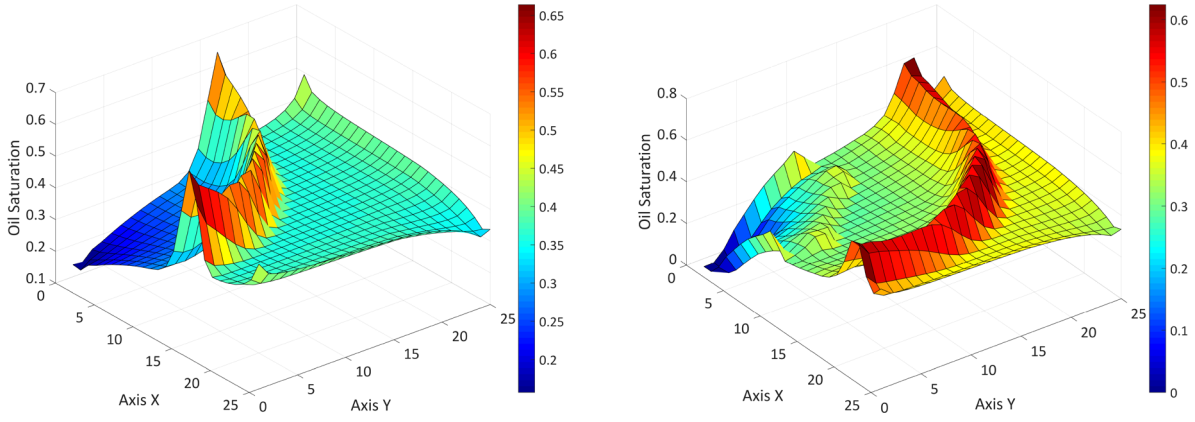

Figure 22. Oil saturation profile after 250 (left) and 500 days (right) of SP flooding starting after a critical fractional flow of $f_f = 0.99$.

adapt the surface facilities accordingly for future EOR operations. Surfactant/polymer flooding showed the potential of chemical EOR methods to sweep the residual oil by means of combining the interfacial properties of surfactants, reducing the IFT, and viscosifying the viscoelastic properties of the polymers. However, it is advised that future research is necessary in order to determine a more complex set of formulations aimed at evaluating the properties affected by the presence of both chemicals acting together.

■ ASSOCIATED CONTENT

Supporting Information

The Supporting Information is available free of charge on the ACS Publications website at DOI: 10.1021/acs.energyfuels.8b02900.

Surfactant−polymer flooding, influence of the injection scheme: optimum SP case with no adsorption and combined secondary and tertiary processes (PDF)

■ AUTHOR INFORMATION

Corresponding Author

*E-mail: f.picchioni@rug.nl. Phone: +31 50 3634333. Fax: +31 50 3634479.

ORCID

Pablo Druetta: 0000-0002-1303-5566

Francesco Picchioni: 0000-0002-8232-2083

Notes

The authors declare no competing financial interest.

■ ACKNOWLEDGMENTS

P.D. thanks the Roberto Rocca Education Program and the Erasmus Mundus EURICA scholarship program (2013-2587/001-001-EMA2) for support.

■ NOMENCLATURE

Ad = component adsorption [1/day]
c_r = rock compressibility [1/Pa]
$\underline{D}$ = dispersion tensor
dm = molecular diffusion [m^2/s]
dl = longitudinal dispersion [m^2/s]
dt = transversal dispersion [m^2/s]
K = absolute permeability [mD]
k_r = relative permeability
p = reservoir pressure [Pa]
p_{wf} = bottomhole pressure [Pa]
q = flow rate [m^3/day]
r_w = well radius [m]
S = phase saturation
s = well skin factor
u = Darcy velocity [m/day]
V = volumetric concentration
z = overall concentration

■ GREEK LETTERS

Γ = domain boundary
δ_{ij} = Kronecker delta

DOI: 10.1021/acs.energyfuels.8b02900
Energy Fuels 2018, 32, 12231−12246

λ = phase mobility [$m^2/(Pa \times s)$]
μ = absolute viscosity [Pa × s]
σ = interfacial tension [mN/m]
ϕ = formation porosity
Ω = reservoir domain

SUPERSCRIPTS

a = aqueous phase
c = capillary
H = water−oil system (no chemical)
j = phase
<*n*> = time step
o = oleous phase
r = residual

SUBSCRIPTS

c = surfactant component
i = component
in = injection
m, *n* = spatial grid blocks
p = petroleum component
pol = polymer component
s = salt component
t = total
w = water component

REFERENCES

(1) Owen, N. A.; Inderwildi, O. R.; King, D. A. The status of conventional world oil reserves-Hype or cause for concern? *Energy Policy* **2010**, *38*, 4743−4749.
(2) Miller, R. G. The Global Oil System - the Relationship between Oil Generation, Loss, Half-Life, and the World Crude-Oil Resource. *AAPG Bull.* **1992**, *76*, 489−500.
(3) Alekkett, K. Peak Oil and the Evolving Strategies of Oil Importing and Exporting Countries: Facing the Hard Truth about an Import Decline for the OECD countries. *Discussion Paper No. 2007−2017*; Joint Transport Research Centre: 2007.
(4) Campbell, C.; Laherrere, J. Preventing the next oil crunch - The end of cheap oil. *Sci. Am.* **1998**, *278*, 77−83.
(5) Laherrere, J. Oil peak or Plateau? *ASPO France*. St. Andrews Economy Forum: France, 2009.
(6) Dake, L. P. *Fundamentals of Reservoir Engineering*, 1st ed.; Elsevier: Amsterdam, The Netherlands, 1978.
(7) Pargman, D.; Eriksson, E.; Hook, M.; Tanenbaum, J.; Pufal, M.; Wangel, J. What if there had only been half the oil? Rewriting history to envision the consequences of peak oil. *Energy Research & Social Science* **2017**, *31*, 170−178.
(8) Maggio, G.; Cacciola, G. When will oil, natural gas, and coal peak? *Fuel* **2012**, *98*, 111−123.
(9) Chapman, I. The end of Peak Oil? Why this topic is still relevant despite recent denials. *Energy Policy* **2014**, *64*, 93−101.
(10) Hughes, L.; Rudolph, J. Future world oil production: growth, plateau, or peak? *Current Opinion in Environmental Sustainability* **2011**, *3*, 225−234.
(11) Lake, L. W.; Schmidt, R. L.; Venuto, P. B. A Niche for Enhanced Oil Recovery in the 1990's. *Oilfield Review* **1992**, *4*, 55−61.
(12) Ahmed, T. *Reservoir Engineering Handbook*; Gulf Publishing Company: Houston, USA, 2000.
(13) Sheng, J. *Modern Chemical Enhanced Oil Recovery*; Elsevier: Amsterdam, The Netherlands, 2011.
(14) Lake, L. W. *Enhanced Oil Recovery*; Prentice-Hall Inc: Englewood Cliffs, USA, 1989.
(15) Satter, A.; Iqbal, G. M.; Buchwalter, J. L. *Practical Enhanced Reservoir Engineering*; PennWell Books: Tulsa, USA, 2008.
(16) Hirasaki, G. J.; Miller, C. A.; Puerto, M. Recent Advances in Surfactant EOR. *SPE Journal* **2011**, *16*, 889−907.
(17) Goddard, E. Polymer/surfactant interaction: Interfacial aspects. *J. Colloid Interface Sci.* **2002**, *256*, 228−235.
(18) Panmai, S.; Prud'homme, R.; Peiffer, D.; Jockusch, S.; Turro, N. Interactions between hydrophobically modified polymers and surfactants: A fluorescence study. *Langmuir* **2002**, *18*, 3860−3864.
(19) Ji, Y.; Wang, D.; Cao, X.; Guo, L.; Zhu, Y. Both-branch amphiphilic polymer oil displacing system: Molecular weight, surfactant interactions and enhanced oil recovery performance. *Colloids Surf., A* **2016**, *509*, 440−448.
(20) Cao, X.-L.; Li, J.; Yang, Y.; Zhang, J.-C.; Zhang, Le.; Zhang, Lu; Zhao, S. Effects of Surfactants on Interfacial Shear Rheological Properties of Polymers for Enhanced Oil Recovery. *Acta Physico-Chimica Sinica* **2014**, *30*, 908−916.
(21) Alzahid, Y.; Mostaghimi, P.; Warkiani, M. E.; Armstrong, R. T.; Joekar-Niasar, V.; Karadimitriou, N. Alkaline Surfactant Polymer Flooding: What Happens at the Pore Scale. *Society of Petroleum Engineers* **2017**, 1.
(22) Feng, A.; Zhang, G.; Ge, J.; Jiang, P.; Pei, H.; Zhang, J.; Li, R. Study of Surfactant-Polymer Flooding in Heavy Oil Reservoirs. *Society of Petroleum Engineers* **2012**, 1.
(23) Marliere, C.; Wartenberg, N.; Fleury, M.; Tabary, R.; Dalmazzone, C.; Delamaide, E. Oil Recovery in Low Permeability Sandstone Reservoirs Using Surfactant-Polymer Flooding. *Society of Petroleum Engineers* **2015**, 1.
(24) Jain, N.; Trabelsi, S.; Guillot, S.; McLoughlin, D.; Langevin, D.; Letellier, P.; Turmine, M. Critical aggregation concentration in mixed solutions of anionic polyelectrolytes and cationic surfactants. *Langmuir* **2004**, *20*, 8496−8503.
(25) Gupta, S. P.; Trushenski, S. P. Micellar Flooding - Compositional Effects on Oil Displacement. *SPEJ, Soc. Pet. Eng. J.* **1979**, *19*, 116−128.
(26) Kumar, B. Effect of Salinity on the Interfacial Tension of Model and Crude Oil Systems. MSc. Thesis, University of Calgary, Canada, 2012.
(27) Al-Sahhaf, T.; Elkamel, A.; Suttar Ahmed, A.; Khan, A. The influence of temperature, pressure, salinity, and surfactant concentration on the interfacial tension of the N-octane-water system. *Chem. Eng. Commun.* **2005**, *192*, 667−684.
(28) Liu, S. Alkaline Surfactant Polymer Enhanced Oil Recovery Process. Ph.D. Thesis, Rice University, Houston, TX, USA, 2007.
(29) Samanta, A.; Ojha, K.; Sarkar, A.; Mandal, A. Surfactant and surfactant-polymer flooding for enhanced oil recovery. *Advances in Petroleum Exploration and Development* **2011**, *2*, 13−18.
(30) Yan, L.; Cui, Z.; Song, B.; Pei, X.; Jiang, J. Dioctyl Glyceryl Ether Ethoxylates as Surfactants for Surfactant-Polymer Flooding. *Energy Fuels* **2016**, *30*, 5425−5431.
(31) Kamal, M. S.; Shakil Hussain, S. M.; Sultan, A. S. Development of Novel Amidosulfobetaine Surfactant-Polymer Systems for EOR Applications. *J. Surfactants Deterg.* **2016**, *19*, 989−997.
(32) Mandal, A. Chemical flood enhanced oil recovery: a review. *Int. J. Oil, Gas Coal Technol.* **2015**, *9*, 241−264.
(33) Hongyan, W.; Xulong, C.; Jichao, Z.; Aimei, Z. Development and application of dilute surfactant-polymer flooding system for Shengli oilfield. *J. Pet. Sci. Eng.* **2009**, *65*, 45−50.
(34) Taiwo, O. A.; Olafuyi, O. A. Surfactant and Surfactant-Polymer Flooding for Light Oil: a Gum Arabic Approach. *Petroleum & Coal* **2015**, *57* (3), 205−215.
(35) Sheng, J. J. Critical review of alkaline-polymer flooding. *J. Pet. Explor. Prod. Technol.* **2017**, *7*, 147−153.
(36) Bataweel, M. A.; Nasr-El-Din, H. A. ASP vs. SP Flooding in High Salinity/Hardness and Temperature in Sandstone Cores. *Society of Petroleum Engineers* **2012**, 1.
(37) Bataweel, M. A.; Nasr-El-Din, H. A. Rheological Study for Surfactant-Polymer and Novel Alkali-Surfactant-Polymer Solutions. *Society of Petroleum Engineers* **2012**, 1.
(38) Xu, X.; Saeedi, A.; Liu, K. An experimental study of combined foam/surfactant polymer (SP) flooding for carbone dioxide-enhanced oil recovery (CO_2-EOR). *J. Pet. Sci. Eng.* **2017**, *149*, 603−611.

DOI: 10.1021/acs.energyfuels.8b02900
Energy Fuels 2018, 32, 12231−12246

(39) Bidner, M. S.; Savioli, G. B. On the Numerical Modeling for Surfactant Flooding of Oil Reservoirs. *Mecanica Computacional* **2002**, *XXI*, 566−585.
(40) Sweatman, R. E.; Crookshank, S.; Edman, S. Outlook and Technologies for Offshore CO_2 EOR/CCS Projects. *Offshore Technology Conference* **2011**, 1.
(41) Chen, Z.; Huan, G.; Ma, Y. *Computational Methods for Multiphase Flows in Porous Media* **2006**, 1.
(42) Druetta, P.; Tesi, P.; De Persis, C.; Picchioni, F. Methods in Oil Recovery Processes and Reservoir Simulation. *Adv. Chem. Eng. Sci.* **2016**, *6*, 39.
(43) Druetta, P.; Yue, J.; Tesi, P.; De Persis, C.; Picchioni, F. Numerical modeling of a compositional flow for chemical EOR and its stability analysis. *Applied Mathematical Modelling* **2017**, *47*, 141−159.
(44) Druetta, P.; Picchioni, F. Numerical Modeling and Validation of a Novel 2D Compositional Flooding Simulator Using a Second-Order TVD Scheme. *Energies* **2018**, *11*, 2280.
(45) Bear, J. *Dynamics of Fluids In Porous Media*; American Elsevier Publishing Company: New York, USA, 1972.
(46) Kuzmin, D. *A guide to numerical methods for transport equations*; University Erlangen-Nuremberg: Germany, 2010.
(47) Barrett, R.; Berry, M.; Chan, T.; Demmel, J.; Donato, J.; Dongarra, J.; Eijkhout, V.; Pozo, R.; Romine, C.; Van der Vorst, H. *Templates for the Solution of Linear Systems: Building Blocks for Iterative Methods*; Society for Industrial and Applied Mathematics: 1994.
(48) Kamalyar, K.; Kharrat, R.; Nikbakht, M. Numerical Aspects of the Convection-Dispersion Equation. *Pet. Sci. Technol.* **2014**, *32*, 1729−1762.
(49) Larson, R. G. The Influence of Phase Behavior on Surfactant Flooding. *SPEJ, Soc. Pet. Eng. J.* **1979**, *19*, 411−422.
(50) Porcelli, P.; Bidner, M. Simulation and Transport Phenomena of a Ternary 2-Phase Flow. *Transp. Porous Media* **1994**, *14*, 101−122.
(51) Attwood, D.; Florence, A. T. *Surfactant Systems−Their Chemistry, Pharmacy and Biology*; Chapman and Hall: London, U.K., 1983.
(52) Delshad, M.; Pope, G.; Sepehrnoori, K. Technical Documentation. *UTCHEM version 9*; The University of Texas at Austin, Austin, USA, 2000.
(53) Hirasaki, G. J. Application of the Theory of Multicomponent, Multiphase Displacement to 3-Component, 2-Phase Surfactant Flooding. *SPEJ, Soc. Pet. Eng. J.* **1981**, *21*, 191−204.
(54) Bidner, M.; Porcelli, P. Influence of phase behavior on chemical flood transport phenomena. *Transp. Porous Media* **1996**, *24*, 247−273.
(55) Bidner, M.; Porcelli, P. Influence of capillary pressure, adsorption and dispersion on chemical flood transport phenomena. *Transp. Porous Media* **1996**, *24*, 275−296.
(56) Khan, M. Y.; Samanta, A.; Ojha, K.; Mandal, A. Interaction between aqueous solutions of polymer and surfactant and its effect on physicochemical properties. *Asia-Pac. J. Chem. Eng.* **2008**, *3*, 579−585.
(57) Ma, B.-D.; Gao, B.-Y.; Zhang, L.; Gong, Q.-T.; Jin, Z.-Q.; Zhang, L.; Zhao, S. Influence of Polymer on Dynamic Interfacial Tensions of EOR Surfactant Solutions. *J. Appl. Polym. Sci.* **2014**, *131*, 40562.
(58) Zhang, L.; Wang, X.-C.; Yan, F.; Luo, L.; Zhang, L.; Zhao, S.; Yu, J.-Y. Interfacial dilational properties of partly hydrolyzed polyacrylamide and gemini surfactant at the decane-water interface. *Colloid Polym. Sci.* **2008**, *286*, 1291−1297.
(59) Ye, Z.; Guo, G.; Chen, H.; Shu, Z. Interaction between Aqueous Solutions of Hydrophobically Associating Polyacrylamide and Dodecyl Dimethyl Betaine. *J. Chem.* **2014**, *2014*, 1.
(60) Camilleri, D.; Engelson, S.; Lake, L. W.; Lin, E. C.; Ohnos, T.; Pope, G.; Sepehrnoori, K. Description of an improved compositional micellar/polymer simulator. *SPE Reservoir Eng.* **1987**, *2*, 427−432.
(61) Camilleri, D.; Fil, A.; Pope, G. A.; Rouse, B. A.; Sepehrnoori, K. Comparison of an improved compositional micellar/polymer simulator with laboratory corefloods. *SPE Reservoir Eng.* **1987**, *2*, 441−451.
(62) Ghannam, M. T.; Hasan, S. W.; Abu-Jdayil, B.; Esmail, N. Rheological properties of heavy & light crude oil mixtures for improving flowability. *J. Pet. Sci. Eng.* **2012**, *81*, 122−128.

DOI: 10.1021/acs.energyfuels.8b02900
Energy Fuels 2018, 32, 12231−12246